2024 IEEE 63rd Conference on Decision and Control (CDC)
December 16-19, 2024. MiCo, Milan, Italy

Pseudospectral collocation for safe optimal motorcycle trajectories

Martin Pryde[1], Lamri Nehaoua[1], Samer Alfayad[1], Hicham Hadj-Abdelkader[1], Hichem Arioui[1]

***Abstract*— The authors investigate the problem of generating safe motorcycle trajectories intended to advise novice riders on how to safely navigate commonly-encountered road geometries. The method solves a nonlinear program using Legendre-Gauss-Radau pseudospectral collocation with a cost function designed to penalize trajectories that novices find challenging to follow. Trajectories are generated for three different motorcycles navigating the following scenarios: a lane change on a straight at $130\,\mathrm{km/h}$, entry and exit of a constant bend at $50\,\mathrm{km/h}$, and traversing a chicane at $80\,\mathrm{km/h}$. The results are compared with those generated by approaches in previous literature and insights are drawn on safe maneuvering for novice riders.**

***Index Terms*— Automotive systems, Optimal control, Optimization algorithms**

I. INTRODUCTION

Motorcycle riders continue to face a disproportionate risk of injury or death compared to other motorists. This disparity has been exacerbated by improvements in automobile safety thanks in part to the widespread introduction of *Advanced Driver Assistance Systemes* (ADAS). Motivated by closing this gap in road safety, researchers at the IBISC laboratory of the University of Paris-Saclay, among others, have been investigating technologies that might one day give rise to similar aids for riders. This concept has been coined by industry as *Advanced Rider Assistance Systems* (ARAS).

A. Motivation

Looking past the accident risk factors motorcyclists share with other motorists, such as intoxication, reckless speeding and inattention to other road users, it becomes clear that inexperience is a significant factor [1], particularly in bends: A motorcycle permits a far larger lateral motion envelope than a car hence it is less obvious to a rider where to position themself to safely negotiate a turn. This risk is compounded by improper cornering, with road exit accidents frequently due to understeering and slideouts caused by overbraking [2]. One recent study [3] investigating the steering behavior of riders of varying levels of experience performed on instrumented motorcycles offers some insight into a possible cause for this improper cornering: it found that novices are hesitant towards maneuvers involving strong lateral accelerations.

B. Problem statement

This paper investigates methods of generating motorcycle trajectories that at once permit the vehicle to safely negotiate a bend while at the same time minimize the aforementioned factors that may unsettle an inexperienced rider. The aspiration is that such methods could comprise a part of an instructive ARAS which would advise the rider on the best trajectory to take through a bend in real-time.

C. Related works

Following his seminal 1971 paper on motorcycle stability, Robin Sharp proposed in 2006 one of the first optimal control schemes for motorcycles based on LQR preview control [4]. In 2010, Biral proposed a system that would alert a rider to unsafe deviations from a previewed trajectory generated by solving an *Optimal Control Problem* (OCP) [5]. This system approximated the motorcycle dynamics to a simple rolling wheel and minimized a cost function designed around rider comfort, from which the costate equations were formed analytically and a *Two-Point Boundary Value Problem* (TPBVP) was solved to generate the optimal trajectory.

In the mid 2010s, there was growing interest in solving *minimum lap time* OCPs for cars [6]. Increasingly sophisticated dynamical models formulated in *curvillinear* coordinates on 2-D and 3-D roads were used to plan trajectories over entire racetracks rather than on a preview horizon.

The works of Limebeer [7] applied *Pseudospectral collocation* methods to minimum lap time OCPs, which reformulate TPBVP OCPs into *NonLinear Programs* (NLPs). These have the advantage of faster convergence times compared to the previous approaches which solved costate equations numerically while still preserving their discrete first-order optimality conditions.

In [8], a Pseudospectral collocation method is used to solve a minimum lap time OCP for a motorcycle model on a 3-D track. The model used here is considerably more sophisticated than a rolling wheel and accounts for steering kinematics and tire forces.

In summary, the current state of the art in motorcycle trajectory generation is still primarily concerned with minimum lap time racing scenarios and there is a lack of research into applying the methods developed for these to the problem of generating safe trajectories for riders on public roads.

D. Contributions

The main contribution of this paper is a method for generating safe motorcycle trajectories intended to advise and instruct novices on how to safely navigate commonly encountered road geometries. The method solves an NLP using the *Legendre-Gauss-Radau* (LGR) pseudospectral collocation method to minimize a cost function designed to penalize trajectories that novices find challenging to follow.

*These works were supported by l'Angence Nationale de la Recherche under project eMC2 N° ANR-22-CE22-0012.

[1]Authors are affiliated with Laboratoire IBISC, Université d'Évry-Val-d'Essonne, Université Paris-Saclay, 36 Rue du Pelvoux, CE 1455 Courcouronnes 91020 Évry Cédex, France, martin.pryde@univ-evry.fr

II. MOTORCYCLE MODELING

An OCP relies on a dynamic system model, balancing fidelity with computational tractability. For safe motorcycle trajectories, capturing traction, cornering, and steering kinematics is vital. The model should accurately represent these while tempering complexity for numerical stability and solution time. Hence, this work focuses solely on lateral dynamics on 2-D roads at fixed longitudinal speeds.

A. The Sharp model

Considering the above, the authors chose the Sharp model [9]. Compared to the model in [8], it uses a linear tire model and neglects aerodynamic loads. Despite this, [10] shows that the Sharp model adequately captures the lateral dynamics in constant longitudinal speed scenarios. A full derivation of the *Linear Parameter-Varying* (LPV) model (1) is given in [11]. The varying parameter is body longitudinal velocity v_x. The constant parameters of $\mathbf{A}$ and $\mathbf{B}$ are listed in Table I.

$$\dot{\boldsymbol{x}}(t) = \mathbf{A}(v_x)\,\boldsymbol{x}(t) + \mathbf{B}\tau_\delta(t) \tag{1}$$

The states $\boldsymbol{x}(t)$ are lean $\varphi(t)$, steering angle $\delta(t)$, body lateral velocity $v_y(t)$, yaw, lean and steering rates $\omega_\psi(t)$, $\omega_\varphi(t)$ and $\omega_\delta(t)$, and rear and front lateral tire forces $Y_r(t)$ and $Y_f(t)$ The control input is the steering torque $\tau_\delta(t)$. Henceforth, the time dependence is neglected for brevity.

$$\boldsymbol{x} = \begin{bmatrix}\varphi & \delta & v_y & \omega_\psi & \omega_\varphi & \omega_\delta & Y_r & Y_f\end{bmatrix}^{\mathrm{T}} \tag{2}$$

B. Curvilinear coordinates

The boundary conditions on vehicle position are not easily expressed in Cartesian coordinates on curving roads. If one models the road centerline as a parametric curve $\mathcal{C} = \mathcal{C}(s)$ with arclength s and instantaneous curvature κ then it is more natural to express the vehicle's pose with respect to this curve. This is achieved through the introduction of the curvilinear coordinates s, the *lateral offset* d and *relative heading* ξ (see Fig. 1). The dynamics of these new states are obtained by expressing the motorcycle's body velocity in $\mathfrak{R}_{\text{rd}}$, noting that $\dot{\xi} = \omega_\psi - \kappa\dot{s}$ and solving for their rates.

An OCP is considerably easier to solve when the boundary values of the independent variable are given. While this is not convenient with time t, when planning trajectories across fixed road geometries it is straightforward with s. For any state q, [12] shows that $q(s) = q(t)$ and by the chain rule $\dot{q} = \dot{s}q'$ where q' is the rate of q with respect to s.

$$\dot{s} = -\frac{v_x\cos(\xi) - v_y\sin(\xi)}{d\kappa - 1} \tag{3}$$

$$\dot{d} = v_y\cos(\xi) + v_x\sin(\xi) \tag{4}$$

$$\dot{\xi} = \omega_\psi + \frac{\kappa\left(v_x\cos(\xi) - v_y\sin(\xi)\right)}{d\kappa - 1} \tag{5}$$

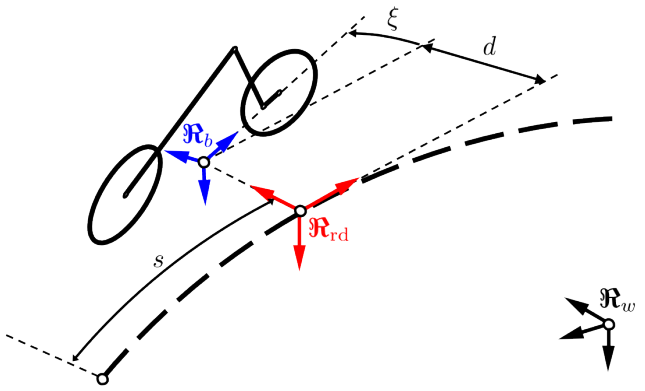

Fig. 1: Curvilinear coordinates: $\mathfrak{R}_{\text{rd}}$ is a *Frenet-Serret* frame following $\mathfrak{R}_b$ whilst constrained to $\mathcal{C}$. The East axis of $\mathfrak{R}_{\text{rd}}$ is normal to $\mathcal{C}$ and always points to the origin of $\mathfrak{R}_b$. The shortest distance between the origins of $\mathfrak{R}_b$ and $\mathfrak{R}_{\text{d}}$ is d and $\xi = \psi - \psi_{\text{rd}}$. Hence, the angular velocity of $\mathfrak{R}_{\text{rd}}$ is $\omega_{\text{rd}} = \kappa\dot{s}$.

C. Curvilinear Sharp model

Combining (1) with (4-5) and exchanging t for s yields the *Curvilinear Sharp model* $\mathbf{x}' = \mathbf{f}(\mathbf{x}, \mathbf{u}, \mathbf{p})$ with the augmented state vector $\mathbf{x} = \begin{bmatrix}d & \xi & \boldsymbol{x}^{\mathrm{T}} & \tau_\delta\end{bmatrix}^{\mathrm{T}}$. Note τ_δ is now a state. This is because the control for the model is the steering torque rate $\mathbf{u} = j_\delta = \dot{\tau}_\delta$ for reasons explained later. The varying parameters $\mathbf{p}$ now include κ as well as v_x. Finally, the rates with respect to s are found by dividing through the system dynamics by (3):

$$\mathbf{f}(\mathbf{x}, \mathbf{u}, \mathbf{p}) = \begin{bmatrix} -\dfrac{(d\kappa - 1)\left(v_y\cos(\xi) + v_x\sin(\xi)\right)}{v_x\cos(\xi) - v_y\sin(\xi)} \\ \dfrac{\omega_\psi - d\kappa\omega_\psi}{v_x\cos(\xi) - v_y\sin(\xi)} - \kappa \\ \dfrac{1}{\dot{s}}\left(\mathbf{A}(v_x)\,\boldsymbol{x} + \mathbf{B}\tau_\delta\right) \\ -\dfrac{j_\delta(d\kappa - 1)}{v_x\cos(\xi) - v_y\sin(\xi)} \end{bmatrix} \tag{6}$$

III. SAFE MOTORCYCLE TRAJECTORIES

Consider the OCP cost function (7) where $\mathscr{M}$ is the terminal cost or *Mayer* term penalizing the initial and final states and times while $\mathscr{L}$ is the running cost or *Lagrange* term penalizing the states and controls over the trajectory:

$$\mathscr{J} = \mathscr{M}(t_0, \boldsymbol{x}_0, t_f, \boldsymbol{x}_f) + \int_{t_0}^{t_f} \mathscr{L}(\boldsymbol{x}, \boldsymbol{u}, t)\,\mathrm{d}t \tag{7}$$

The initial and final states are known in the scenarios considered in Section V. Additionally, recall from Section II-A that v_x is constant hence there is no need to numerically motivate the motorcycle to reach the final state. Thus, the Mayer term is neglected and after a change of independent variable to s the Lagrange term becomes $\mathscr{L} = \mathscr{L}(\mathbf{x}, \mathbf{u}, s)$.

A. Lateral tire forces

The safest trajectory minimizes the risk of loss of control of the vehicle. Recall from Section I-A that new riders avoid strong lateral accelerations to the detriment of proper cornering. In motorcycles, lateral acceleration is generated by the lateral tire forces Y_r and Y_f. The authors first attempted to implement a simple quadratic cost on Y_r and Y_f. However, it was observed that this resulted in peak magnitudes higher than if this cost was not included. This is undesirable for traction even if the average magnitude is lower. Hence, the authors propose instead to penalize the force rates $\dot{Y}_r$ and $\dot{Y}_f$ whose values are obtained from (1). These rates must be reformulated to match the independent variable using (3). Note that using rates with respect to s necessitates that κ is now a variable in the cost function (15) as it is for (6).

$$\mathscr{L}_Y = Q_Y \left(\left(Y_r'\right)^2 + \left(Y_f'\right)^2 \right) \tag{8}$$

B. Understeering and oversteering

Another accident risk mentioned in Section I-A is understeering and oversteering. In both the relaxation length and the more ubiquitous *Pacejka* tire models, lateral tire force is a function of the rear and front tire *slip* angles, α_r and α_f, as well as the rear and front *camber* γ_r and γ_f. Sharp provides approximations for the former where b is the aft wheelbase given in Table I and l is the forward wheelbase derived from the Sharp parameters as $l = (a - a_n) / \cos(\varepsilon)$.

$$\alpha_r = \frac{b\omega_\psi - v_y}{v_x} \tag{9}$$

$$\alpha_f = \delta \cos(\varepsilon) - \frac{v_y + l\omega_\psi - a_n\omega_\delta}{v_x} \tag{10}$$

Cossalter hypothesizes the following conditions (11-13) to determine the steering behavior of a motorcycle [13]. The last condition is the slip angles are equal and the motorcycle is said to be steering *kinematically*, meaning cornering behavior is determined only by the rider's steering torque inputs.

$$\alpha_r \leq \alpha_f \therefore \text{understeering} \tag{11}$$

$$\alpha_r > \alpha_f \therefore \text{oversteering} \tag{12}$$

$$\alpha_r = \alpha_f \therefore \text{neutral steering} \tag{13}$$

While experienced riders can exploit oversteer for faster cornering, a novice will prefer the predictability of kinematic steering. Hence, the authors propose a second running cost on the lateral slip where $\Delta\alpha = \alpha_r - \alpha f$:

$$\mathscr{L}_\alpha = Q_\alpha \Delta\alpha^2 \tag{14}$$

C. Cost function

Gathering (8-14) and summing yields the total running cost $\mathscr{L}(\mathbf{x}, \mathbf{u})$ where the constants Q_Y, Q_α and Q_u are the weights assigned to each term.

$$\mathscr{L}(\mathbf{x}, \mathbf{u}, \mathbf{p}) = Q_Y \left(\left(Y_r'\right)^2 + \left(Y_f'\right)^2 \right) + Q_\alpha \Delta\alpha^2 \tag{15}$$

D. Rejected cost functions

Other cost functions were considered and rejected beyond the aforementioned cost on $Y_{r,f}$. A cost on lean rate ω_φ was considered in order to penalize sudden leaning maneuvers, however in tests this resulted in violent oscillations across trajectories. A direct cost on lateral velocity to minimize the magnitude of body slip had a similar effect on tire force peak values as rejected lateral force cost. Other costs were found to be redundant: it is common to include a cost on the control input, however the use of lateral tire force rates in (8) already incorporates this term.

IV. DIRECT COLLOCATION

A *Direct collocation* (DC) method reformulates an OCP as an NLP where the state and control are *transcribed* into a set of decision variables evaluated at discrete intervals of the independent variable called *collocation points*:

$$t \to t_0, t_1, \ldots, t_N \tag{16}$$

$$\boldsymbol{x}(t) \to \boldsymbol{x}_0, \boldsymbol{x}_1, \ldots, \boldsymbol{x}_N \tag{17}$$

$$\boldsymbol{u}(t) \to \boldsymbol{u}_0, \boldsymbol{u}_1, \ldots, \boldsymbol{u}_N \tag{18}$$

For review, consider the general *Hamitonian* of an OCP (19) where $\boldsymbol{\lambda}$ are the Lagrange multipliers called *costates* involved in minimizing (7) subject to the plant dynamics:

$$\mathscr{H}(\boldsymbol{x}, \boldsymbol{u}, \boldsymbol{\lambda}, t) = \mathscr{L}(\boldsymbol{x}, \boldsymbol{u}, t) + \boldsymbol{\lambda}^{\mathrm{T}} \mathbf{f}(\boldsymbol{x}, \boldsymbol{u}, t) \tag{19}$$

Excluding transversality conditions for brevity, the necessary conditions for optimality as mentioned in Section I-C are the *Hamilton canonical equations*:

$$\dot{\boldsymbol{x}} = \frac{\partial \mathscr{H}(\boldsymbol{x}, \boldsymbol{u}, \boldsymbol{\lambda}, t)}{\partial \boldsymbol{\lambda}} \tag{20}$$

$$\dot{\boldsymbol{\lambda}} = -\frac{\partial \mathscr{H}(\boldsymbol{x}, \boldsymbol{u}, \boldsymbol{\lambda}, t)}{\partial \boldsymbol{x}} \tag{21}$$

$$\mathbf{0} = \frac{\partial \mathscr{H}(\boldsymbol{x}, \boldsymbol{u}, \boldsymbol{\lambda}, t)}{\partial \boldsymbol{u}} \tag{22}$$

Where the optimal control $\boldsymbol{u}^\star$ obtained from (22) is some function of the states and costates. The main advantage of DC methods over indirect methods, such as shooting methods and dynamic programming, is that they do not need to solve for nor require an initial guess of costate trajectories assuming no analytical solution to (20-22) exists.

A. Pseudospectral collocation

The state of the art in DC are the *PseudoSpectral* (PS) methods. Especially popular are the Legendre family of methods [14], whose collocation points $\tau \in [-1, 1]$ are the roots of a function of Legendre polynomials $P_N(\tau)$.

$$P_N(\tau) = \frac{1}{2^N} \sum_{k=0}^{\lfloor N/2 \rfloor} (-1)^k \binom{N}{k} \binom{2(N+k)}{k} \tau^{N-2k} \tag{23}$$

This family comprises the original Legendre-Gauss (LG), the *Legendre-Gauss-Radau* (LGR) and the *Legendre-Gauss-Lobatto* (LGL) methods. These methods differ primarily on which points on τ are collocated [15]. Conversion from this interval to $s \in [s_0, s_f]$ is possible using the following:

$$s = \left(\frac{s_f - s_0}{2}\right)\tau + \frac{s_0 + s_f}{2} \tag{24}$$

The authors implemented all three for the scenarios described in Section V: LG converged to smooth trajectories in all cases but did so slowly in some instances. LGL failed to converge in many cases. Possible explanations are provided in [16] where LG requires additional quadrature constraints to satisfy in order to incorporate the final state while the LGL *Gauss Pseudospectral Differentation* (GPD) matrix is singular. For these reasons, the authors selected LGR for the remainder of this work.

B. Legendre-Gauss-Radau collocation

Each state in $\mathbf{x}$ is approximated by a *Lagrange polynomial* with basis $\boldsymbol{l}_k = \boldsymbol{l}(\tau_k)$ where $k \in [1, N]$. An efficient way to compute all the bases $\mathbf{L} = \begin{bmatrix}\boldsymbol{l}_1 & \cdots & \boldsymbol{l}_N\end{bmatrix}$ is using the *Vandermonde matrix* $\mathbf{V}$ up to $\tau_{N+1} = 1$. Hence, it becomes trivial to obtain the GPD matrix $\mathbf{D}$ by differentiation of $\mathbf{L}$ with respect to τ_k:

$$\mathbf{V} = \begin{bmatrix} 1 & \tau_1 & \tau_1^2 & \cdots & \tau_1^N \\ 1 & \tau_2 & \tau_2^2 & \cdots & \tau_2^N \\ \vdots & \vdots & \vdots & \ddots & \vdots \\ 1 & \tau_{N+1} & \tau_{N+1}^2 & \cdots & \tau_{N+1}^N \end{bmatrix} \tag{25}$$

$$\mathbf{L} = \mathbf{V}^{-\mathrm{T}} \begin{bmatrix} 1 & 1 & \cdots & 1 \\ \tau_0 & \tau_1 & \cdots & \tau_N \\ \tau_0^2 & \tau_1^2 & \cdots & \tau_N^2 \\ \vdots & \vdots & \ddots & \vdots \\ \tau_0^N & \tau_1^N & \cdots & \tau_N^N \end{bmatrix} \tag{26}$$

$$\mathbf{D} = \mathbf{V}^{-\mathrm{T}} \begin{bmatrix} 0 & 0 & \cdots & 0 \\ 1 & 1 & \cdots & 1 \\ 2\tau_0 & 2\tau_1 & \cdots & 2\tau_N \\ \vdots & \vdots & \ddots & \vdots \\ N\tau_0^{N-1} & N\tau_1^{N-1} & \cdots & N\tau_N^{N-1} \end{bmatrix} \tag{27}$$

Now the decision variables $\mathbf{X} = \begin{bmatrix}\mathbf{x}_1 & \cdots & \mathbf{x}_N\end{bmatrix}$ and $\mathbf{U} = \begin{bmatrix}\mathbf{u}_1 & \cdots & \mathbf{u}_N\end{bmatrix}$, as well as the transcribed varying parameters $\mathbf{P} = \begin{bmatrix}\mathbf{p}_1 & \cdots & \mathbf{p}_N\end{bmatrix}$, are gathered. Define the augmented state matrix $\overline{\mathbf{X}} = \begin{bmatrix}\mathbf{x}_1 & \cdots & \mathbf{x}_{N+1}\end{bmatrix}$. Now assemble the *collocation constraints* using (27) and the plant dynamics where $\Delta s = (s_f - s_0)/2$:

$$\overline{\mathbf{X}}\mathbf{D} = \Delta s \mathbf{F}(\mathbf{X}, \mathbf{U}, \mathbf{P}) \tag{28}$$

Gauss-Radau quadrature is used to compute the running cost where $\mathbf{w}$ are the weights for all k as listed [15]:

$$J(\mathbf{X}, \mathbf{U}) = \Delta s \mathbf{w}^{\mathrm{T}} L(\mathbf{X}, \mathbf{U}, \mathbf{P}) \tag{29}$$

Upon solving the NLP, the trajectories are interpolated across the whole (continuous) interval $\tau \in [-1, 1]$ with the same method used in (26) i.e. $\mathbf{x}(\tau) = \mathbf{X}\boldsymbol{l}(\tau)$.

C. Nonlinear program

Some risks are mitigated by imposing boundary conditions on certain states e.g. requiring that the vehicle stays on the road is accomplished by imposing a maximum lateral offset $d_{\max}$. The tire profiles permit a maximum lean $\varphi_{\max}$. A rider can only apply so much steering torque $\tau_{\delta_{\max}}$. Thus, the complete NLP is as follows:

$$\min \quad J(\mathbf{X}, \mathbf{U}) = \Delta s \mathbf{w}^{\mathrm{T}} L(\mathbf{X}, \mathbf{U}, \mathbf{P}) \tag{30}$$

$$\text{s.t.} \quad \overline{\mathbf{X}}\mathbf{D} = \Delta s \mathbf{F}(\mathbf{X}, \mathbf{U}, \mathbf{P}) \tag{31}$$

$$\mathbf{x}_0 = \mathbf{x}(s_0) \tag{32}$$

$$\mathbf{x}_{N+1} = \mathbf{x}(s_f) \tag{33}$$

$$-d_{\max} \leq d \leq d_{\max} \tag{34}$$

$$-\varphi_{\max} \leq \varphi \leq \varphi_{\max} \tag{35}$$

$$-\tau_{\delta_{\max}} \leq \tau_\delta \leq \tau_{\delta_{\max}} \tag{36}$$

V. DRIVING SCENARIOS

Three scenarios were chosen (see Fig. 4). All roads have boundaries of $\mp 3.5\,\mathrm{m}$. The first is a lane change $\mp 1.75\,\mathrm{m}$ over a $125\,\mathrm{m}$ straight at $130\,\mathrm{km/h}$. The second is a $90°$ bend of radius $50\,\mathrm{m}$ with a $50\,\mathrm{m}$ straight at each end entered and exited with zero offset at $50\,\mathrm{km/h}$. The third is a chicane composed of two connected $100\,\mathrm{m}$ *clothoids* with infinite end radii and $\frac{150}{\pi}\mathrm{m}$ radii at their connection (see Fig. 4c). The motorcycle enters and exits with zero offset along $25\,\mathrm{m}$ straights at $80\,\mathrm{km/h}$. For the latter two scenarios, the initial and final lateral offset were left free to be optimized.

A. Motorcycles

Three motorcycles were used in each scenario. Their physical parameters were adapted from models provided in BikeSim®. These models are of interest as their parameters have been selected to resemble typical examples of real motorcycles. The values for each are given in Table I.

The first motorcycle shown in Fig. 3a is the *Big sports* type. It has the smallest *caster* angle ε of the three which should render it the most maneuverable. The second shown in Fig. 3b is the *Cruiser* type. It has the largest caster and *trail* a_n inferring that it is the least maneuverable but the most stable. The last shown in Fig. 3c is the *Touring* type. It is the heaviest with caster and trail comparable to Big sports.

VI. RESULTS

The NLP was implemented in MATLAB and solved using CasADI with IPOPT. The degree of polynomial selected for each scenario was $N = 38$, the highest the implementation could achieve without numerical rootfinding issues. The authors decided against a multistage approach to LGR collocation due to the simple road geometries and to avoid discontinuities in the generated trajectories. With constant v_x, the only varying parameter provided to the solver τ_k is the

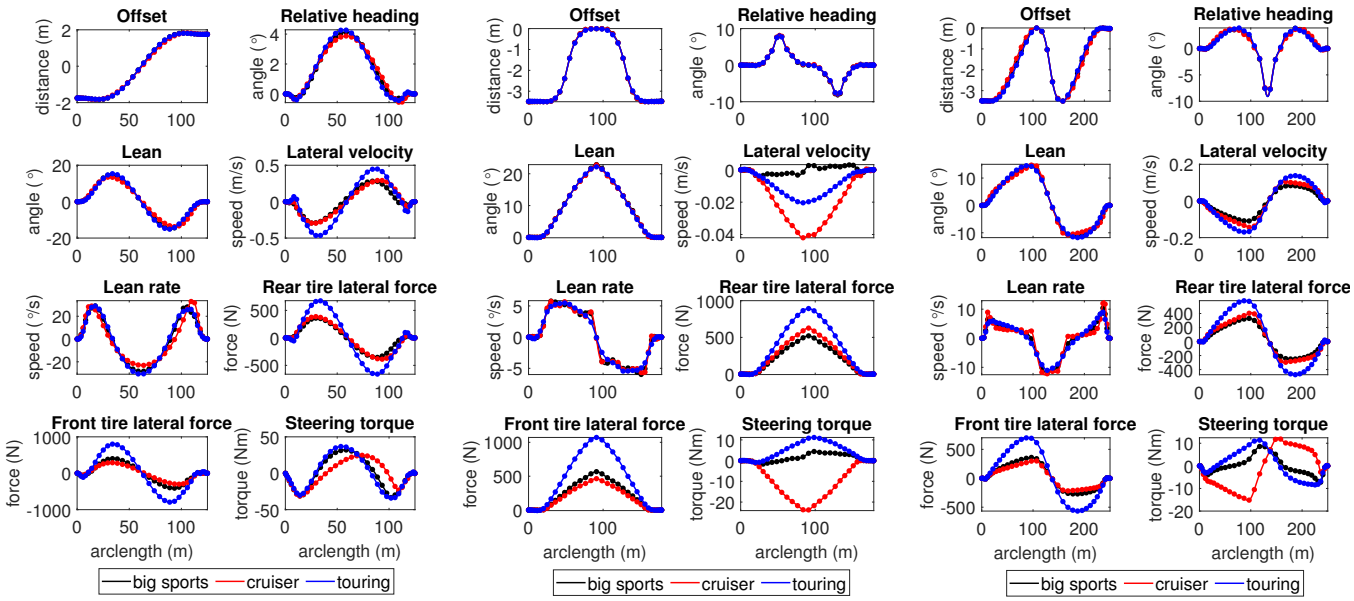

(a) Straight trajectories (b) Arc trajectories (c) Chicane trajectories

Fig. 2: Trajectories for each motorcycle type in each scenario: Dots represent collocation points.

(a) Big sports (b) Cruiser (c) Touring

Fig. 3: Motorcycles used in the scenarios

TABLE I: Sharp parameters for the three motorcycles

Parameter	Big sports	Cruiser	Touring
C_δ	12.6738	12.1582	12.1582
C_{f1}	20566	18022	24931
C_{f2}	908.1083	745.0421	1745
C_{r1}	20174	21959	24689
C_{r2}	648.8377	762.6843	1131.3
C_{rxz}	-2.1731	-3.152	4.8623
I_{fx}	1.8204	2.6789	3.454
I_{fz}	0.6908	1.4436	1.8398
I_{rx}	19.6528	17.4187	38.4762
I_{rz}	30.9076	26.3416	65.834
Z_f	-1357.8	-1625.9	-2371.3
a	0.7525	0.9287	0.7658
a_n	0.0882	0.1279	0.0657
b	0.6429	0.573	0.8636
e	0.0253	0.0499	0.0563
f	0.2344	0.2125	0.2653
g	9.81	9.81	9.81
h	0.575	0.5592	0.4505
i_{fy}	0.484	0.484	0.6
i_{ry}	0.638	0.638	0.9
m_f	24.24	24.24	27.24
m_r	257.06	257.19	495.3600
r_f	0.282	0.318	0.313
r_r	0.297	0.321	0.313
σ	0.1979	0.098	0.1949
ε	0.4189	0.5934	0.5061

road curvature i.e. $\mathbf{P} = \begin{bmatrix}\kappa_1 & \cdots & \kappa_N\end{bmatrix}$ (see Section IV-B). The cost function weights from Section III-C were chosen first to scale the state units with subsequent modifications to improve the trajectory smoothness. They were set to $Q_Y = 1\text{e}-9$ and $Q_\alpha = 1\text{e}5$ respectively.

A. *Straight scenario*

Examining Fig. 2a, Touring has the highest lateral velocity indicating it is slipping the most, perhaps due to its significantly larger mass. Note in the steering torque for all three motorcycles that the optimal control is the *countersteering* maneuver where the rider steers away from the intended direction of travel at the start and the end of the maneuver. Cruiser's torque lags Big sports and Touring and is compressed towards the end which is an expected result of the large caster and trail mentioned in Section V-A.

B. *Arc scenario*

A *racing line* profile is evident when examining Fig. 4b and Fig. 2b. However, unlike a pure racing line, the lean trajectories here adopt a slightly triangular form. The lean rates hint toward a more bang-bang profile, especially notable for Touring. Big sports slips the least and requires the least steering torque, an expected result due to its smaller caster. Cruiser copes the worst in this scenario with the highest slip and twice the required steering torque compared to Touring despite weighing half as much.

C. *Chicane scenario*

A racing line path is once again observed in the Chicane scenario as shown in Fig. 4c. Countersteering is less apparent here due to the smooth transition curve properties of the clothoid segments. Touring slips the most as in the straight scenario shown in Figure 2a.

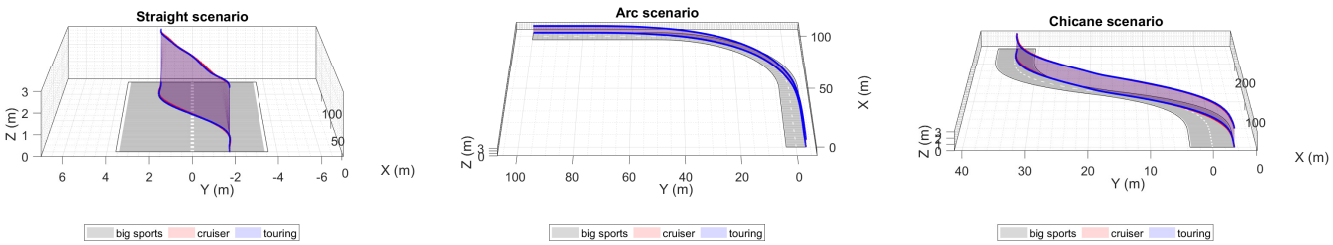

(a) Straight scenario (b) Arc scenario (c) Chicane scenario

Fig. 4: Road geometries for each scenario with superimposed lean and offset profiles for each motorcycle

VII. DISCUSSION

A noteworthy result across scenarios is similar offset and lean, inferring that the safest of these profiles do not vary greatly from one motorcycle to the next. One explanation is that each vehicle has a similar rear chassis mass center height h: If the motorcycle is approximated as a traveling inverted pendulum then the lean dynamics are far more sensitive to differences in h than in inertial parameters.

A. Comparison with related works

The results concur with [8] demonstrating the racing line. This is not unexpected: The racing line maximizes turning radius therefore minimizing the centripetal forces acting on the tires. Furthermore, converting from time to arclength in (8) has implicitly introduced the term $1/\dot{s}$ into the cost function which is what one would seek to minimize when optimizing for minimum time. However, there are important differences: Minimizing lateral force rates rather than input torques as in [8] has resulted in reductions of peak values of up to 20 N. When the slip cost (14) is added this saving can reach 100 N. The results also differ greatly from those in [5] whose simple model follows the spine of the road despite also having a cost function designed around rider safety.

VIII. CONCLUSION

This work has addressed a gap in motorcycle trajectory generation research. The authors considered recent studies into the steering behavior of novice riders and consulted theory to develop a cost function prioritizing rider safety. The OCP was solved using pseudospectral collocation for a range of motorcycles and scenarios. The implementation generated smooth trajectories that converged in under 1 s and were consistent with theoretical understanding. The results provide insights into where novices should position themselves on the road and how they should lean to stabilize a turn.

A. Future work

The trajectories generated here should be evaluated on a nonlinear plant with a Pacejcka tire model in BikeSim®. Longitudinal dynamics should be introduced into the model to investigate the safety of overtaking manoeuvers. Since no rider is capable of perfect tracking, *reachability* of the trajectories should be investigated to determine how far a rider can stray from the recommended path before endangering themselves. This future study will aim to compute a tube-like *safety envelope* for the rider to remain within to provide a more robust recommendation.

REFERENCES

[1] A. H. Goodwin, Y. C. Wang, R. D. Foss, and B. Kirley, "The role of inexperience in motorcycle crashes among novice and returning motorcycle riders," *Journal of Safety Research*, vol. 82, pp. 371–375, 2022.

[2] H. H. Hurt, J. V. Ouellet, and D. R. Thom, "Motorcycle accident cause factors and identification of countermeasures," National Highway Traffic Safety Administration (NHTSA), resreport 81-1, Jan. 1981. [Online]. Available: https://rosap.ntl.bts.gov/view/dot/6450

[3] M. Bartolozzi, A. Boubezoul, S. Bouaziz, G. Savino, and S. Espié, "Understanding the behaviour of motorcycle riders: An objective investigation of riding style and capability," *Transportation Research Interdisciplinary Perspectives*, vol. 22, p. 100971, 2023.

[4] R. S. Sharp, "Optimal linear time-invariant preview steering control for motorcycles," *Vehicle System Dynamics*, vol. 44, no. 1, pp. 329–340, 2006.

[5] F. Biral and M. D. Lio, "An intelligent curve warning system for powered two wheel vehicles," *European Transport Research Review*, 2010.

[6] R. Lot and F. Biral, "A Curvilinear Abscissa Approach for the Lap Time Optimization of Racing Vehicles," *IFAC Proceedings Volumes*, vol. 47, no. 3, pp. 7559–7565, 2014.

[7] D. J. N. Limebeer and G. Perantoni, "Optimal Control of a Formula One Car on a Three-Dimensional Track—Part 2: Optimal Control," *Journal of Dynamic Systems, Measurement, and Control*, vol. 137, no. 5, 05 2015, 051019.

[8] L. Leonelli and D. J. N. Limebeer, "Optimal control of a road racing motorcycle on a three-dimensional closed track," *Vehicle System Dynamics*, vol. 58, no. 8, pp. 1285–1309, 2020.

[9] R. S. Sharp, "The Stability and Control of Motorcycles," *Journal of Mechanical Engineering Science*, vol. 13, no. 5, pp. 316–329, 1971.

[10] L. Nehaoua, D. Ichalal, H. Arioui, J. Davila, S. Mammar, and L. M. Fridman, "An unknown-input hosm approach to estimate lean and steering motorcycle dynamics," *IEEE Transactions on Vehicular Technology*, vol. 63, no. 7, pp. 3116–3127, Sep. 2014.

[11] R. Lot and M. D. Lio, "A Symbolic Approach for Automatic Generation of the Equations of Motion of Multibody Systems," *Multibody System Dynamics*, vol. 12, pp. 147–172, Sep. 2004.

[12] F. Biral, E. Bertolazzi, and D. L. Mauro, *The Optimal Manoeuvre*. John Wiley & Sons, 2014, ch. 5, pp. 119–154.

[13] V. Cossalter, *Motorcycle Dynamics*, 2nd ed. Lulu, Oct. 2006.

[14] D. Garg, M. Patterson, W. Hager, A. Rao, D. R. Benson, and G. T. Huntington, "An overview of three pseudospectral methods for the numerical solution of optimal control problems," Oct. 2017, working paper or preprint. [Online]. Available: https://hal.science/hal-01615132

[15] P. J. Davis and I. Polonsky, *Handbook of Mathematical Functions With Formulas, Graphs, and Mathematical Tables*, 9th ed., ser. Applied Mathematics. National Bureau of Standards, Dec. 1972, vol. 55, ch. Numerical Interpolation, Differentiation and Integration, pp. 887–888.

[16] M. Patterson, "Efficient solutions to nonlinear optimal control problems usingadaptive mesh orthogonal collocation methods," Ph.D. dissertation, University of Florida, May 2013. [Online]. Available: https://ufdcimages.uflib.ufl.edu/uf/e0/04/52/36/00001/patterson_m.pdf